

## Eugenol treatment delays the flesh browning of fresh-cut water chestnut (*Eleocharis tuberosa*) through regulating the metabolisms of phenolics and reactive oxygen species

Lijuan Zhu<sup>a,b,c</sup>, Wanfeng Hu<sup>a,b,c,\*</sup>, Ayesha Murtaza<sup>a,b,c</sup>, Aamir Iqbal<sup>a,b,c</sup>, Jiaying Li<sup>a,b,c</sup>, Jiao Zhang<sup>a,b,c</sup>, Junjie Li<sup>a,b,c</sup>, Mengjie Kong<sup>a,b,c</sup>, Xiaoyun Xu<sup>a,b,c</sup>, Siyi Pan<sup>a,b,c</sup>

<sup>a</sup> College of Food Science and Technology, Huazhong Agricultural University, Wuhan 430070, China

<sup>b</sup> Key Laboratory of Environment Correlative Dietology (Huazhong Agricultural University), Ministry of Education, China

<sup>c</sup> Hubei Key Laboratory of Fruit & Vegetable Processing & Quality Control (Huazhong Agricultural University), Wuhan, Hubei 430070, China

### ARTICLE INFO

#### Keywords:

Water chestnut  
Eugenol  
Browning  
Phenylalanine ammonia-lyase  
Reactive oxygen species metabolism  
Phenolics metabolism  
Molecular docking

### ABSTRACT

The potential mechanism behind the browning inhibition in fresh-cut water chestnuts (FWC) after eugenol (EUG) treatment was investigated by comparing the difference in browning behavior between surface and inner tissues. EUG treatment was found to inactivate browning-related enzymes and reduce phenolic contents in surface tissue. Molecular docking further confirmed the hydrophobic interactions and hydrogen bonding between EUG and phenylalanine ammonia-lyase (PAL). Moreover, EUG also enhanced reactive oxygen species (ROS)-scavenging enzyme activities, ultimately decreasing the O<sub>2</sub><sup>-</sup> generation rates. Regarding inner tissue, EUG induced the accumulation of colorless phenolic compounds and increased the antioxidant capacity. In conclusion, 1.5 % EUG exhibited the best inhibitory effect on FWC browning, which partly attribute to the direct inhibitory effects on PAL activity. Furthermore, EUG could also enhance the enzymatic/non-enzymatic antioxidant capacity and alleviate the ROS damage to membranes, thereby, preventing the contact between oxidative enzymes and phenols and indirectly inhibiting the enzymatic browning in FWC.

### 1. Introduction

Water chestnuts (*Eleocharis tuberosa*) are cultivated worldwide, including American, Africa and Asia, with China as one of the largest producer in the world with total production around 800, 000 tons a year (Song et al., 2019a). The peeled corms of water chestnuts are mostly eaten raw owing to its unique, fresh taste and high nutritional value (Pan, Li, & Yuan, 2015). Although, fresh-cut water chestnut (FWC) is one of the most consumed fresh-cut products in China, but the cut-edge tissue of FWC is prone to yellowing which could result in shorter shelf life (He & Pan, 2017). Previous studies reported phenylalanine ammonia-lyase (PAL) as the critical enzyme which involved in the yellowing of FWC (Kong et al., 2021; Song et al., 2019a; Teng et al., 2020). Besides, the accumulation of flavonoids (not oxidation products of phenolic compounds) also led to the yellowing of FWC (Pan et al., 2015).

The production of phenolic compounds in wounded tissue might be the main cause of browning in FWC. Moreover, the enzymatic oxidation of phenolic compounds by polyphenol oxidase (PPO) and peroxidase (POD) could also contribute to the discoloration of FWC.

Apart from enzymes, postharvest browning of fruit and vegetables is considered to be associated with the reactive oxygen species (ROS) metabolism (Chen et al., 2019; Zhang et al., 2018). Biotic and abiotic stimuli (e.g. mechanical damage) could also induce the overproduction of ROS (superoxide anion (O<sub>2</sub><sup>-</sup>) and hydrogen peroxide) in plant tissue (Finkel, 2011). The overproduction of ROS could lead to the membrane lipid peroxidation, further causing extensive damage to the cell membrane (Das & Roychoudhury, 2014). Hence, the loss of sub-cellular compartmentalization might lead to the contact between oxidative enzymes (including PPO and POD) and phenolic compounds, ultimately, resulting in the enzymatic browning of fruit and vegetables (Zhang et al.,

**Abbreviations:** FWC, Fresh-cut water chestnut; EUG, Eugenol; ROS, Reactive oxygen species; PAL, Phenylalanine ammonia-lyase; PPO, Polyphenol oxidase; POD, Peroxidase; TPC, Total phenols content; BI, Browning index; PBS, Sodium phosphate buffer; MDA, Malondialdehyde; SOD, Superoxide dismutase; CAT, Catalase; APX, Ascorbate peroxidase; T-AOC, Total antioxidant capacities; MIO, 4-methylidene-imidazole-5-one.

\* Corresponding author.

E-mail address: [wanfenghu@mail.hzau.edu.cn](mailto:wanfenghu@mail.hzau.edu.cn) (W. Hu).

<https://doi.org/10.1016/j.fochx.2022.100307>

Received 5 February 2022; Received in revised form 4 April 2022; Accepted 7 April 2022

Available online 9 April 2022

2590-1575/© 2022 The Authors. Published by Elsevier Ltd. This is an open access article under the CC BY-NC-ND license (<http://creativecommons.org/licenses/by-nc-nd/4.0/>).

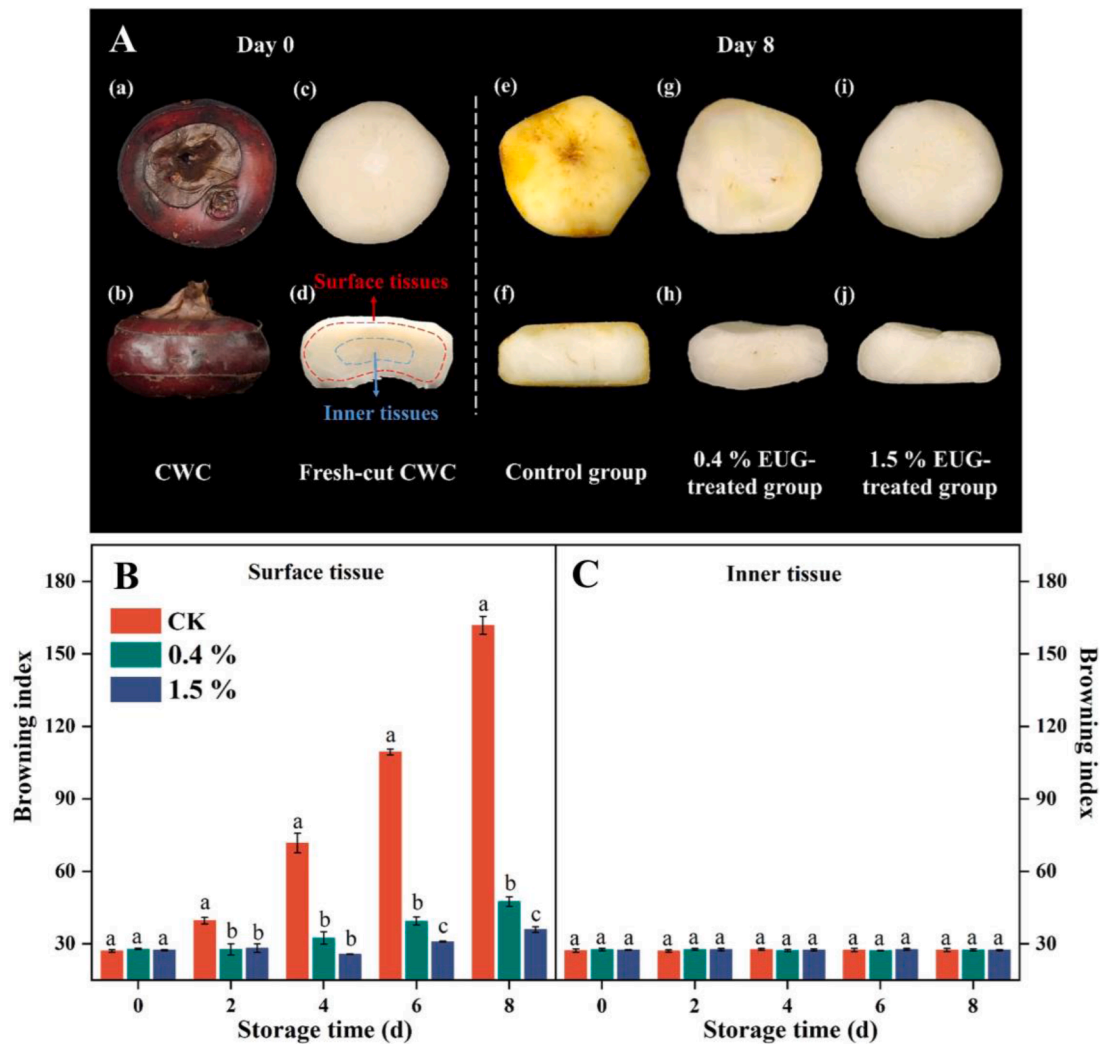


**Fig. 1.** (A) Color change of fresh-cut water chestnut after eight days of storage: (a) vertical view of water chestnut; (b) side view of water chestnut; (c) vertical view of fresh-cut water chestnut on day 0; (d) profile of fresh-cut water chestnut on day 0; (e) vertical view of control group on day 8; (f) profile of control group on day 8; (g) vertical view of 0.4 % eugenol-treated group on day 8; (h) profile of 0.4 % EUG-treated group on day 8; (i) vertical view of 1.5 % eugenol-treated group on day 8; (j) profile of 1.5 % EUG-treated group on day 8. (B) Changes in browning indexes of surface tissue in fresh-cut water chestnut after eugenol treatment (0 %, 0.4 % and 1.5 %). (C) Changes in browning indexes of inner tissue in fresh-cut water chestnut after eugenol treatment. Bars represent standard deviation of the mean. Different lowercase letters above the bars within the same storage time indicate significant difference at  $P < 0.05$  level ( $t$ -test).

2018). Several studies found that the higher antioxidant activity had positive impacts on inhibiting the browning reactions in fresh-cut blueberries (Chen et al., 2019), fresh-cut pineapples (Jing, Huang, & Yu, 2019) and fresh-cut sweet potatoes (Pan et al., 2020). Some studies also suggested that the short term anoxia treatment (You et al., 2012), hydrogen sulfide (Dou et al., 2021), and hydrogen-rich water (Li et al., 2022) could also inhibit the enzymatic browning in FWC by enhancing the antioxidant activity.

Eugenol (4-allyl-2-methoxy-phenol, EUG) is the main component of clove essential oil and has several health-promoting activities such as antioxidative and antibacterial properties (Sharifimehr, Soltanizadeh, & Goli, 2019). EUG is an FDA (Food and Drug Administration) approved food additive, with  $LD_{50}$  value of  $3000 \text{ mg kg}^{-1}$  oral mouse (Gong et al., 2016). EUG has been considered to impart a great positive role in the postharvest preservation of fruit and vegetables because of its natural taste and safe final products. Besides having antibacterial and antifungal properties in EUG, several studies also found the potential application of EUG in inhibiting the browning in fresh-cut products (Chen et al., 2017; Teng et al., 2020; Wieczynska & Cavoski, 2018). Based our previous study, EUG was found to have positive effects on inhibiting flesh browning in FWC. Currently, various chemical agents (such as ferulic

acid (Song et al., 2019b), hydrogen sulfide (Dou et al., 2021), and hydrogen-rich water (Li et al., 2022)) were used to prevent tissue browning in FWC. EUG is preferred to hydrogen sulfide due to its safety and various health benefits. Compared to ferulic acid and hydrogen-rich water, EUG is favored because of its low production costs (Martinez-Hernandez et al., 2019). Hence, the usage of EUG for inhibiting browning in fresh-cut could be technically and economically beneficial. However, the possible mechanism behind the browning inhibition after EUG treatment still remains unclear and should be further investigated for better understanding of the application of natural compounds for the production of fresh-cut fruit and vegetables products.

“Surface tissue” is generally the tissue within 2 mm from the cut surface of FWC, in which the cell integrity is totally destroyed (Kong et al., 2021). While “inner tissue” refers to internal tissue which has intact cellular structures. Surface tissue come into direct contact with oxygen in the environment, inducing the over-production of ROS. Whereas, the inner tissue could undergo a series of secondary metabolism, while responding to the mechanical wounding stress. Therefore, there are huge differences in metabolism between surface tissue and inner tissue. Hence, in this study, FWC was divided into surface and inner tissues to investigate the mechanism of browning inhibition and

ROS metabolism in FWC after EUG treatment.

This study used different concentration of EUG emulsions (with the concentrations of 0.4 % and 1.5 %) to treat FWC to reveal the mechanism of browning inhibition. The effects of EUG treatment on browning-related enzymes (PPO, POD and PAL) and total phenols contents in both surface and inner tissues of FWC were evaluated. In addition, the current study also revealed the effects of EUG treatment on ROS metabolism of FWC by evaluating the changes in ROS-scavenging enzyme activities, antioxidant capacity and  $O_2^-$  generation rate. Furthermore, molecular docking was applied to study the direct interactions between EUG and enzymes such as PAL and superoxide dismutase (SOD). Therefore, this study would provide a better insight in understanding the mechanism of browning inhibition in FWC after EUG treatment and developing a non-toxic means to maintain the visual quality of fresh-cut products.

## 2. Materials and methods

### 2.1. Plant materials and eugenol preparation

Fresh water chestnut (*Eleocharis tuberosa*) cv. Xiaogan with commercial maturity (total soluble solid content 11 % and hardness 65 N) were purchased from a local market in Wuhan, China. The selected water chestnuts were uniform in shape and size (diameters: 4.0 cm; thickness: 2.5 cm; weight: 20 g). Fresh water chestnuts were washed, peeled, and stored at  $4 \pm 1$  °C, without further cutting into small pieces.

EUG (99 % purity) was purchased from Aladdin (Shanghai, China). Based on our previous study, EUG concentrations were set at 0.4 % and 1.5 % (w/v), which were in line with the criterion. 4.5 g EUG was mixed with 1.5 g of Span 80, 28.5 g Tween 80, and then diluted with distilled water to make the final concentrations of 0.4 % and 1.5 %.

### 2.2. Experimental design for eugenol treatment

FWC were randomly separated into three groups (two treated and one control), and then two groups of FWC were dipped into emulsions of 0.4 % and 1.5 % EUG (solutions already prepared with water) for 60 s. Then, all the treated FWC were dried under ambient conditions for 1 h. All of the treated and control samples were packed in the same-sized valve bags (110 mm × 160 mm × 0.08 mm, width × length × thickness). The samples were stored at  $4 \pm 1$  °C for eight days, with 48 h sampling interval. In this study, each FWC sample was then divided into surface and inner tissues. The surface tissue was defined as the tissue within 2 mm from the cut surface, while the inner tissue was defined as the oval internal tissue (long diameter: 20 mm, short diameter: 6 mm, height: 6 mm) (Fig. 1 A-(d)). Surface and inner tissues were immediately sampled and assayed for the following biochemical indexes.

### 2.3. Browning index assays

Color values ( $L^*$ ,  $a^*$  and  $b^*$ ) were measured using a Chroma meter (YS3060, Jiulian Technology Co., Ltd., Suzhou, China). The colorimeter was calibrated against a standard white plate ( $L^* = 100$ ,  $a^* = 0$ ,  $b^* = 0$ ). For each experiment, three replicates, each including six FWC, were used to measure color values. Browning indexes (BI) were calculated by equations (1) and (2) (Feumba et al., 2020).

$$BI = \frac{(x - 0.31) \times 100}{0.172} \quad (1)$$

Where,

$$x = \frac{a^* + 1.75 \times L^*}{5.645 \times L^* + a^* - 3.012 \times b^*} \quad (2)$$

### 2.4. Browning-related enzyme activities assays

Samples (0.3 g derived from six FWC) were ground with 1.5 mL of

sodium phosphate buffer (PBS, 50 mmol L<sup>-1</sup>, pH 6.0) and centrifuged at 10 000 g for 30 min. The reaction system was composed of the supernatant and catechol solution (0.15 mol L<sup>-1</sup>) in a ratio of 1:2 (v/v). One unit (U) of PPO activity was defined as the amount of enzyme causing an increase in  $A_{420}$  of 0.01 per min (Chen et al., 2017). Results were expressed as U kg<sup>-1</sup> on a fresh weight basis. For each experiment, 18 individual FWC were used to measure PPO activity with three replicates.

The preparation method of POD enzyme extraction was the same as that of PPO extraction. The reaction system was composed of the supernatant, H<sub>2</sub>O<sub>2</sub> (2 %) and guaiacol (0.25 mol L<sup>-1</sup>) in a ratio of 1:1:1 (v/v/v). One unit of POD activity was defined as the amount of enzyme that caused an increase in  $A_{470}$  of 0.1 per min, expressed as U kg<sup>-1</sup> (Chen et al., 2017). For each experiment, 18 individual FWC were used to measure POD activity with three replicates.

To determine the value of PAL activity, the samples (0.3 g derived from six FWC) were ground with Tris-HCl buffer (1.5 mL, 100 mmol L<sup>-1</sup>, pH 8.8) containing 40 g L<sup>-1</sup> polyvinylpyrrolidone (PVP), 2 mmol L<sup>-1</sup> ethylene diamine tetra-acetic acid (EDTA), and 5 mmol L<sup>-1</sup> β-mercaptoethanol. After centrifugation at 12 000 g for 30 min, the supernatant was mixed with L-phenylalanine solution (0.02 mol L<sup>-1</sup>) in a ratio of 1:5 (v/v). After incubation at 37 °C for 1.5 h, 0.2 mL of 6 mol L<sup>-1</sup> HCl was added into the reaction system. One unit of PAL activity was defined as the amount of enzyme causing an increase in absorbance at 290 nm per h (Kong et al., 2021). For each experiment, 18 individual FWC were used to measure PAL activity with three replicates.

### 2.5. Total phenols content assays

Water chestnut samples (0.1 g, derived from six FWC) were homogenized with 1.5 mL of 40 % ethanol and centrifuged at 14 000 g for 20 min. The extract (1 mL) and Folin-Ciocalteu reagent (1 mL, 1 mol L<sup>-1</sup>) were mixed, followed by adding 3 mL 7.5 % Na<sub>2</sub>CO<sub>3</sub>. After the incubation of 1 h, the absorbance at 725 nm was measured. The calculation of total phenols contents (TPC) was based on the standard of gallic acid and expressed as g kg<sup>-1</sup> (Perumal, Sellamuthu, Nambiar, & Sadiku, 2017). For each experiment, 18 FWC were used to measure TPC with three replicates.

### 2.6. Total antioxidant capacity assays

Water chestnut tissues (0.25 g, derived from six FWC) were blended with 1 mL normal saline solution. 0.1 mL of extract were diluted with 0.9 mL of 10 % methanol (v/v), and then combined with 1.2 mL of ferric-reducing antioxidant power assay solution containing acetate buffer (1 mL, 300 mmol L<sup>-1</sup>, pH 3.6), 2,4,6-tripyridyl-2-triazine solution (0.1 mL, 10 mmol L<sup>-1</sup>), and FeCl<sub>3</sub> (0.1 mL, 20 mmol L<sup>-1</sup>). The absorbance at 593 nm was recorded after 0 and 6 min. The total-antioxidant capacities (T-AOC) were expressed as g kg<sup>-1</sup> (Kim, Kim, Kim, & Park, 2013). Quercetin was used to draw a standard curve. For each experiment, 18 individual FWC were used to measure T-AOC with three replicates.

### 2.7. O<sub>2</sub><sup>-</sup> generating rate assays

Samples (0.5 g) derived from six FWC were ground with 1 mL of PBS (50 mmol L<sup>-1</sup>, pH 7.8) containing 1 mmol L<sup>-1</sup> EDTA, 1 % PVP, and 0.3 % Triton X-100. After centrifugation at 10 000 g for 20 min, the supernatant was combined with PBS and hydroxylammonium chloride (10 mmol L<sup>-1</sup>) at 25 °C for 20 min. The resulting solution was combined with 4-aminobenzene sulfonic acid (17 mmol L<sup>-1</sup>) and α-naphthylamine (7 mmol L<sup>-1</sup>) for another 20 min. Then, the absorbance was recorded at 530 nm. NaNO<sub>2</sub> was used to draw the standard curve (Sun et al., 2018). O<sub>2</sub><sup>-</sup> generation rate was expressed as mol min<sup>-1</sup> kg<sup>-1</sup>. For each experiment, 18 individual FWC were used to measure O<sub>2</sub><sup>-</sup> generating rate with three replicates.

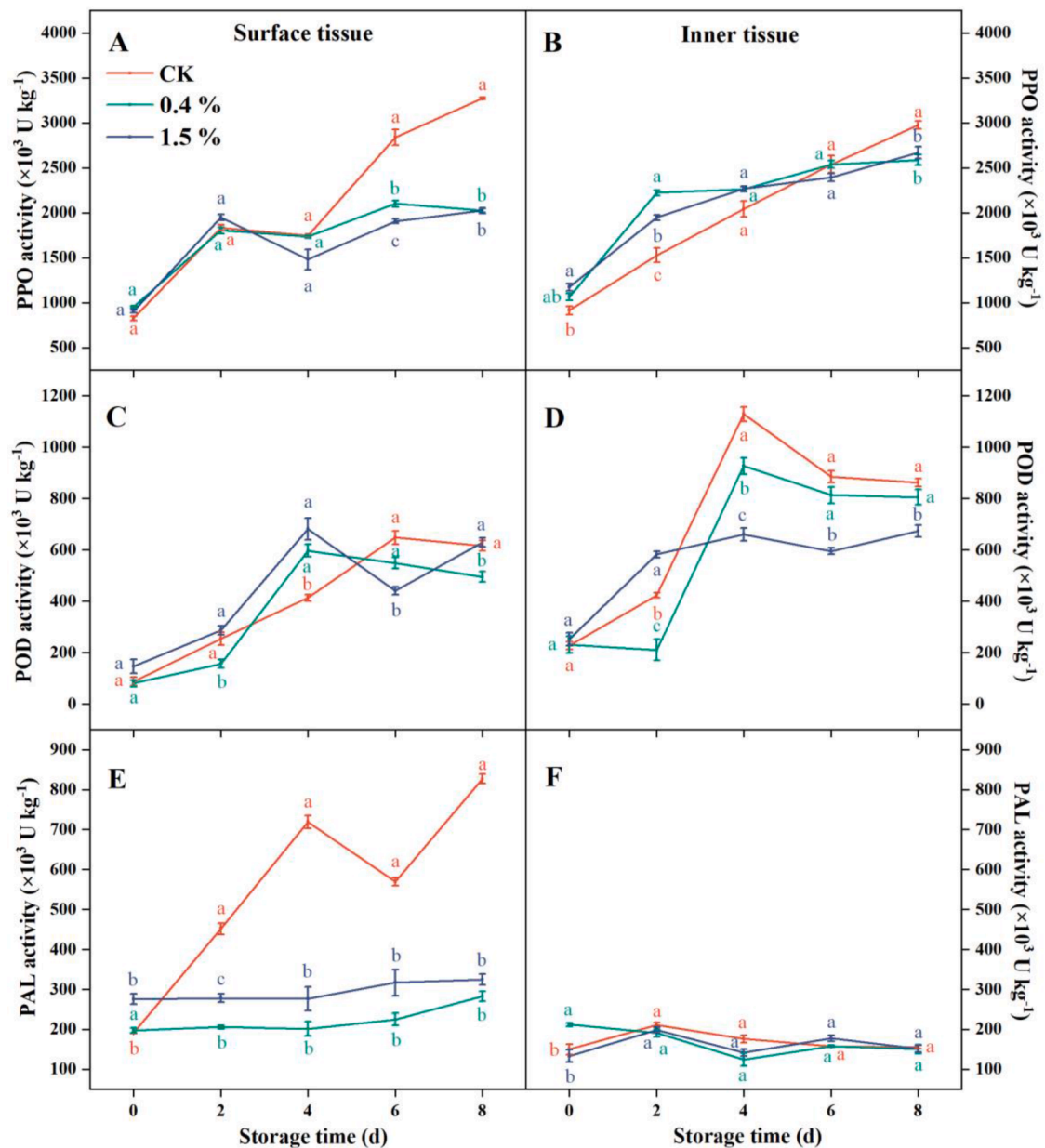


**Fig. 2.** (A) Changes in polyphenol oxidase activities of surface tissue in fresh-cut water chestnut after eugenol treatment (0 %, 0.4 % and 1.5 %). (B) Changes in polyphenol oxidase activities of inner tissue in fresh-cut water chestnut after eugenol treatment. (C) Changes in peroxidase activities of surface tissue in fresh-cut water chestnut after eugenol treatment. (D) Changes in peroxidase activities of inner tissue in fresh-cut water chestnut after eugenol treatment. (E) Changes in phenylalanine ammonia-lyase activities of surface tissue in fresh-cut water chestnut after eugenol treatment. (F) Changes in phenylalanine ammonia-lyase activities of inner tissue in fresh-cut water chestnut after eugenol treatment. Bars represent standard deviation of the mean. Different lowercase letters above the bars within the same storage time indicate significant difference at  $P < 0.05$  level ( $t$ -test).

## 2.8. Malondialdehyde content assays

The samples (0.3 g derived from six FWC) were homogenized in 5 % trichloroacetic acid (1 mL) and then centrifuged (5 000 g) for 20 min. The supernatant was mixed with 0.5 % thiobarbituric acid for 30 min at 95 °C, and then quickly cooled down. The absorbance was recorded at 450, 532 and 600 nm, respectively. Malondialdehyde (MDA) content was calculated by the formula of You et al. (2012). For each experiment, 18 FWC were used to measure MDA content with three replicates.

$$\text{MDA content (mmol kg}^{-1}\text{)} = (6.45 \times (A_{532} - A_{600}) - 0.56 \times A_{450}) \quad (3)$$

Where,  $A_{450}$ ,  $A_{532}$ , and  $A_{600}$  are the absorbance at 450 nm, 532 nm, and 600 nm, respectively.

## 2.9. ROS-scavenging enzymes activities assays

Samples (0.3 g derived from six FWC) were ground in PBS (1.5 mL, 0.05 mol L<sup>-1</sup>, and pH 7.0) containing 2.5 % PVP and 0.1 mmol L<sup>-1</sup> EDTA. The supernatant after centrifugation (12 000 g for 20 min) was used for the assay of superoxide dismutase (SOD) activity. One unit of SOD was defined as the amount of enzyme needed to inhibit 50 % of NBT reduction (Perumal et al., 2017). For each experiment, 18 individual FWC were used to measure SOD activity with three replicates.

The preparation method of catalase (CAT) enzyme extraction was the same as that of SOD extraction. The assay mixture (3 mL) contained 2.45 mL of PBS (0.05 mol L<sup>-1</sup>, pH 7.0), 0.5 mL H<sub>2</sub>O<sub>2</sub> (15 mmol L<sup>-1</sup>) and 0.05 mL extract. One unit of CAT activity was calculated as the amount of enzyme that caused a change in absorbance at 240 nm of 0.01 per min

(Dou et al., 2021). For each experiment, 18 individual FWC were used to measure CAT activity with three replicates.

The ascorbate peroxidase (APX) extraction was obtained by blending tissues (0.5 g derived from six FWC) with PBS (1 mL, 0.05 mol L<sup>-1</sup>, pH 7.5), containing 2.5 % PVP and 0.2 mmol L<sup>-1</sup> ascorbic acid. The reaction mixture consisted of 2.6 mL PBS, 0.45 mL H<sub>2</sub>O<sub>2</sub> (0.1 mmol L<sup>-1</sup>) and 0.1 mL of supernatant. One unit of APX activity was defined as the amount of enzyme causing an increase in A<sub>290</sub> of 0.01 per min (You et al., 2012). For each experiment, 18 individual FWC were used to measure APX activity with three replicates.

### 2.10. Molecular docking

The 3D structures of PAL and SOD of water chestnuts were constructed by homology modeling. The PAL sequence was obtained from National Center for Biotechnology Information (NCBI), and the SOD sequence was obtained from our transcriptomic data. Then, SWISS-MODEL (<https://swissmodel.expasy.org/>) was used to construct PAL and SOD models. Finally, PROCHECK, ERRAT and VERIFY 3D were used to evaluate the models. The evaluation results indicated that the prediction model of PAL and SOD had good accuracy and rationality (Fig. S1 and Fig. S2).

AutoDock Vina was applied for the molecular docking stimulation (Trott & Olson, 2010). The 3D conformer of EUG was downloaded from the PubChem database (<https://pubchem.ncbi.nlm.nih.gov>) with accession ID 3314. The grid coordinates of the binding box of PAL were identified as center x: 123.9, center y: 25.4, and center z: 22.1 with dimensions size x: 15.4, size y: 13.3, and size z: 16.3. The grid coordinates of the binding box of SOD for molecular docking were as center x: 63.0, center y: 29.9, and center z: 18.1 with dimensions size x: 53.1, size y: 78.8, and size z: 48.5. The semi-flexible docking was adopted: the protein structure was kept rigid, and all the torsional bonds of EUG were set free. The optimal binding position of the complex was the model with the lowest binding energy. PyMOL and LigPlot<sup>+</sup> were used to visualize the interactions between enzymes and EUG.

### 2.11. Statistical analysis

All the values were shown as “mean ± standard deviation (SD)” from three independent experiments. Data was analyzed by the analysis of variance using Original 8.5 Pro. Samples *t*-test was performed to investigate the comparison of means with a 95 % significant level.

## 3. Results and discussion

### 3.1. Browning index analysis

FWC in control group turned yellow after 8 d, while there was barely any color change in 1.5 % EUG-treated groups (Fig. 1A). Various techniques were applied to inhibit browning in FWC, mainly including dipping or coating with chemical compounds (You et al., 2012). However, these chemical reagents are generally limited due to their high cost, instable effect, and lack of safety. For example, ascorbic acid, a commonly used anti-browning reagent, couldn't inhibit browning in FWC (Song et al., 2019b). Other chemical compounds, such as hydrogen sulfide (with a concentration of 15 μL L<sup>-1</sup>), could only inhibit around 40 % browning in FWC (Dou et al., 2021). Compared to other known techniques, EUG exhibited a better effect on inhibiting tissue browning in FWC.

Browning index (BI) is considered an important parameter for evaluating the degree of color change (Feumba et al., 2020). As shown in Fig. 1B, BI of the surface tissue in the controlled group showed an obvious increasing trend (from 27.06 ± 0.54 to 161.80 ± 3.73), indicating that untreated FWC underwent severe enzymatic browning. From day 2 to day 8, BI of EUG-treated groups was significantly lower than that of control (*P* < 0.05), proving that EUG treatment could maintain

the visual quality of FWC. Similarly, the profound inhibition of tissue browning by EUG treatment was reported in fresh-cut lettuce (Chen et al., 2017). In addition, from day 6 to day 8 of storage period, BI of 1.5 % EUG-treated group was significantly lower than that of 0.4 % EUG-treated group (*P* < 0.05), indicating that the inhibition effect of EUG treatment on browning was enhanced with the increase of concentration. As shown in Fig. 1C, there was no significant change in BI of inner tissue during storage in both controlled and EUG-treated groups (*P* > 0.05). Several studies have also reported that discoloration only occurs in the surface tissue of FWC (Kong et al., 2021; Li et al., 2022).

### 3.2. Browning-related enzyme activities analysis

Enzymatic browning is one of the most common reactions in the postharvest stage of fruit and vegetables, which involves several enzymes such as PPO, POD and PAL (Kong et al., 2021). PPO can catalyze the oxidation of phenolic compounds to *o*-quinones, which further polymerize into brown pigments (Chen et al., 2017). As shown in Fig. 2A, PPO activities in surface tissue of EUG-treated groups were significantly lower than that of control in the last two days of storage (*P* < 0.05). Fig. 2B showed that EUG treatment could slightly alter the PPO activities in the inner tissue of FWC. POD can also cause enzymatic browning in the presence of H<sub>2</sub>O<sub>2</sub> (Teng et al., 2020). As shown in Fig. 2C and 2D, POD activities in both surface and inner tissues of FWC exhibited an upward tendency within the first four days, and subsequently decreased after 4 days of storage. Interestingly, an obvious reduction in POD activity was noted in the inner tissue of 1.5 % EUG-treated group from day 4 onward. All in all, EUG treatment can reduce the activities of PPO and POD of FWC in late stage of storage. Similar effects of hydrogen sulfide on PPO and POD activities of FWC were also reported in previous studies (Dou et al., 2021). However, according to correlation analysis, there was no significant correlation between BI and PPO/POD activity of FWC (Table S1).

As the principal enzyme of the phenylpropanoid pathway, PAL drives towards the synthesis of phenolic compounds, some of which are substrates for PPO and POD (Liu et al., 2019). As shown in Fig. 2E, PAL activity in the controlled group increased markedly. By contrast, EUG-treated groups showed significantly lower PAL activities than the controlled group from day 2 onward (*P* < 0.05). The effect of EUG treatment on PAL activity in surface tissue of FWC was similar to that of high pressure CO<sub>2</sub> treatment (Kong et al., 2021). In addition, a significant positive correlation was found between BI and PAL activity in 0.4 % and 1.5 % EUG-treated groups (Table S1). Previous literatures have also reported that PAL was closely related to the browning of FWC (Teng et al., 2020). Therefore, it can be concluded that the browning of FWC could be attenuated by the inhibition of PAL activity by EUG treatment. PAL activities in the inner tissue of untreated FWC were kept at a lower level than that in the surface tissue (Fig. 2F). This might be due to the fact that signal molecules induced by wounding cannot be transmitted to inner tissue and therefore cannot trigger the expression of PAL gene and the enhancement of PAL activity (Surjadinata & Cisneros-Zevallos, 2012). As with the control, PAL activities in EUG-treated groups also kept at a low level, suggesting that EUG treatment had no effect on PAL activity in the inner tissue of FWC.

Therefore, EUG treatment could delay the browning of FWC by inhibiting the activities of browning-related enzymes (PPO, POD and PAL). Our study found that EUG treatment had the best inhibition effect on PAL enzyme, which was considered to be the key enzyme leading to the browning in FWC.

### 3.3. Total phenols content and total-antioxidant capacity analysis

Phenolic compounds are important secondary metabolites in plants, which are usually generated by the phenylpropanoid pathway (Boudet, 2007). On the one hand, they have specific antioxidant abilities that enable the plants to adapt to the adversity; on the other hand, they are

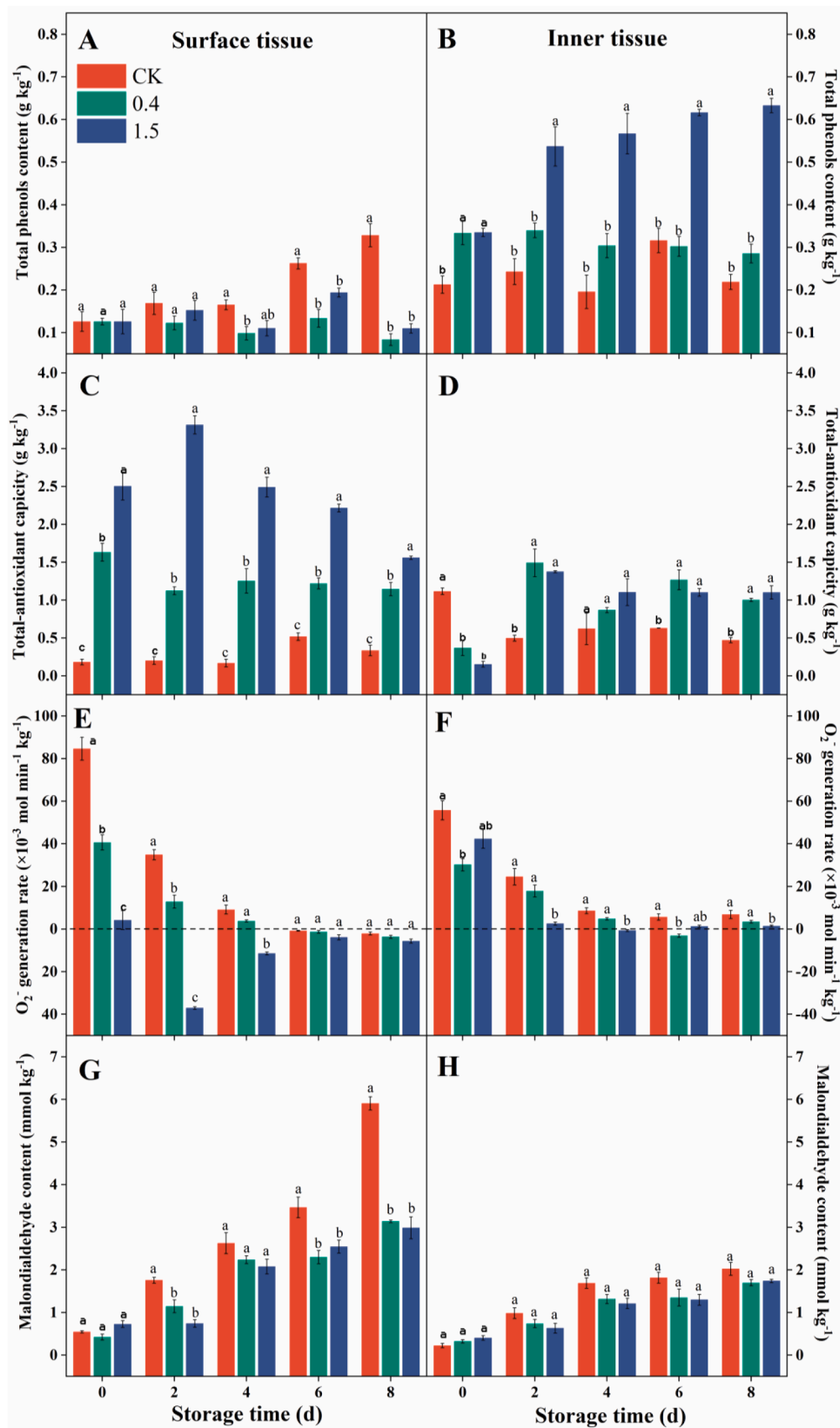


**Fig. 3.** (A) Changes in total phenols contents of surface tissue in fresh-cut water chestnut (FWC) after eugenol (EUG) treatment (0 %, 0.4 % and 1.5 %). (B) Changes in total phenols contents of inner tissue in FWC after EUG treatment. (C) Changes in total-antioxidant capacities of surface tissue in FWC after EUG treatment. (D) Changes in total-antioxidant capacities of inner tissue in FWC after EUG treatment. (E) Changes in O<sub>2</sub><sup>-</sup> generating rate of surface tissue in FWC after EUG treatment. (F) Changes in O<sub>2</sub><sup>-</sup> generating rate of inner tissue in FWC after EUG treatment. (G) Changes in malondialdehyde content of surface tissue in FWC after EUG treatment. (H) Changes in malondialdehyde content of inner tissue in FWC after EUG treatment. Bars represent standard deviation of the mean. Different lowercase letters above the bars within the same storage time indicate significant difference at *P* < 0.05 level (*t*-test).

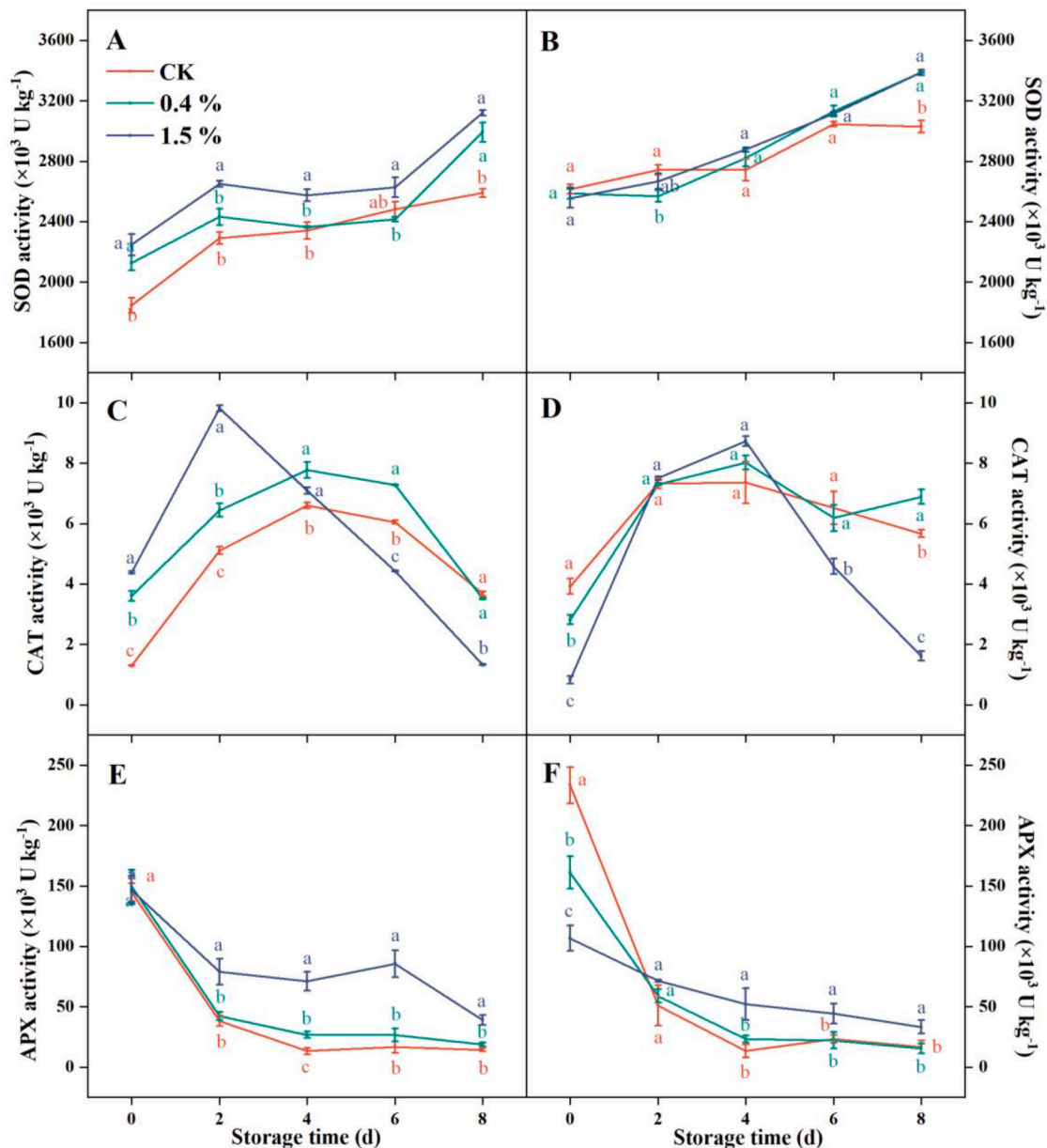


**Fig. 4.** (A) Changes in superoxide dismutase activities of surface tissue in fresh-cut water chestnut after eugenol treatment (0 %, 0.4 % and 1.5 %). (B) Changes in superoxide dismutase activities of inner tissue in fresh-cut water chestnut after eugenol treatment. (C) Changes in catalase activities of surface tissue in fresh-cut water chestnut after eugenol treatment. (D) Changes in catalase activities of inner tissue in fresh-cut water chestnut after eugenol treatment. (E) Changes in ascorbate peroxidase activities of surface tissue in fresh-cut water chestnut after eugenol treatment. (F) Changes in ascorbate peroxidase activities of inner tissue in fresh-cut water chestnut after eugenol treatment. Bars represent standard deviation of the mean. Different lowercase letters above the bars within the same storage time indicate significant difference at  $P < 0.05$  level ( $t$ -test).

the substrates for enzymatic browning (Concellón, Zaro, Chaves, & Vicente, 2012). As shown in Fig. 3A, total phenols content (TPC) during the storage (day 4 - day 8) was significantly lower in EUG-treated groups than that of control ( $P < 0.05$ ), and EUG content had been subtracted from TPC. These results were similar to the variation trend of BI and PAL activity in the surface tissue of FWC (Fig. 1B and Fig. 2E). Therefore, it was found that the content of phenolic compounds was consistent with the browning degree in the surface tissue of FWC, as reported previously (Pan et al., 2015). Moreover, it was also suggested that EUG treatment could delay the discoloration of FWC by inhibiting the generation of yellow phenolic compounds, including eriodictyol and naringenin (Kong et al., 2021). As shown in Fig. 3B, the TPC of 1.5 % EUG-treated samples was significantly higher than that of the controlled and 0.4 % EUG-treated groups ( $P < 0.05$ , EUG content had been subtracted from TPC

in 0.4 % and 1.5 % EUG-treated groups). These results indicated that EUG treatment with a high concentration (1.5 %) could stimulate the accumulation of phenolic compounds in inner tissue of FWC. This finding coincided with the results in honey peach reported by Zhou et al. (2019), wherein EUG could activate phenolic metabolism in peach fruit. Given that there was no color change in inner tissue (Fig. 1C), it was suggested that the phenolic compounds (mainly *p*-hydroxybenzoic acid and chlorogenic acid) accumulated in the inner tissue were colorless or not enough to exhibit yellow (Teng et al., 2020). Whereas, these phenolic compounds were antioxidants and could protect the cell membrane from ROS damage by self-oxidation (Perumal et al., 2017).

Total-antioxidant capacity ( $T$ -AOC) shows the capacity of scavenging ROS and reduce oxidative damage to plant tissue (Chen et al., 2019). As shown in Fig. 3C,  $T$ -AOC of surface tissue in the controlled group

increased slightly on day 6, which might be due to the accumulation of phenolic compounds (Fig. 3A). EUG-treated groups were noted to exhibit significantly higher T-AOC (including the antioxidant capacity of EUG) compared to the controlled group during storage ( $P < 0.05$ ). Besides, the increasing trend of T-AOC in 1.5 % EUG-treated group was observed from day 0 to day 2. The antioxidant capacity of EUG was not enough to explain the effect of EUG treatment on enhancing T-AOC in surface tissue of FWC. Combined with the results in Fig. 4A, C and E, it is suggested that EUG treatment could increase T-AOC of FWC by activating ROS-scavenging enzymes. Similarly, Zeng et al. (2012) reported that 'Newhall' navel orange dipped with clove bud extract (mainly containing EUG) exhibited higher ROS-scavenging enzyme activities and antioxidant capacity. It's noted that T-AOC of 1.5 % EUG-treated group was significantly higher than that of 0.4 % EUG-treated group ( $P < 0.05$ ), indicating that EUG treatment had a concentration-dependent effect on increasing T-AOC of the surface tissue of FWC. As illustrated in Fig. 3D, T-AOC in the inner tissue of EUG-treated groups were significantly higher than that of control from day 2 onward ( $P < 0.05$ ). Given that EUG treatment could increase the TPC in inner tissue (Fig. 3B), it can be inferred that EUG treatment could enhance the T-AOC of inner tissue by inducing the synthesis of phenolic compounds. These results were consistent with the research on blueberries reported by Chen et al. (2019), where the change of antioxidant capacity followed a similar trend as total phenolic compounds. In conclusion, EUG treatment could increase the antioxidant capacity of both surface and inner tissues, thereby effectively alleviating oxidative damage to FWC.

### 3.4. $O_2^-$ generating rate and malondialdehyde content analysis

The generation and accumulation of  $O_2^-$  can cause structural and functional membrane dysfunction (Zhang et al., 2018). As shown in Fig. 3E and 3F, the  $O_2^-$  generation rates in both surface and inner tissues of the control were immediately induced by the cutting process, suggesting that untreated FWC undertook excessive oxidative stress (Farooq et al., 2019).  $O_2^-$  generation rates decreased in the controlled group with the extension of time, which was not consistent with the result that superoxide radical scavenging activity in FWC decreased during storage (You et al., 2012). This might be due to the different cutting methods and experimental operations. From day 0 to day 4,  $O_2^-$  generation rates in surface tissue of the controlled group were significantly higher than that of EUG-treated groups, wherein  $O_2^-$  generation rates in 0.4 % EUG-treated group were significantly higher than that in 1.5 % of EUG-treated group ( $P < 0.05$ , Fig. 3E). It is suggested that EUG treatment has a significant inhibition effect on the generation of  $O_2^-$  in surface tissue, which was enhanced as the concentration increased. As displayed in Fig. 3F,  $O_2^-$  generation rates in inner tissue of control were significantly lower than that of surface tissue on days 0 and 2 ( $P < 0.05$ ), indicating that there was less oxidative stress in inner tissue at an early stage. For inner tissue, it was observed that  $O_2^-$  generation rates in EUG-treated groups were significantly lower than that of the control ( $P < 0.05$ ). Based on these data, it could be speculated that EUG treatment could reduce the generation of  $O_2^-$  in both surface and inner tissues, thereby, alleviating ROS damage and oxidative stress in FWC.

Malondialdehyde (MDA) is the final product of membrane lipid peroxidation, which is an important parameter to evaluate ROS damage to the cell membrane of fruit and vegetables (Sun et al., 2020). As shown in Fig. 3G, MDA contents on days 2, 6 and 8 in surface tissue of EUG-treated groups were significantly lower than that of control ( $P < 0.05$ ), suggesting that EUG treatment could inhibit the membrane lipid peroxidation and maintain the integrity of cell membranes in surface tissue during storage (especially in late stage). You et al. (2012) also reported a similar effect of short-term anoxia treatment on MDA content in FWC. As displayed in Fig. 3H, MDA contents in inner tissue were significantly lower than that in surface tissue during the whole storage ( $P < 0.05$ ), confirming that the lipid peroxidation of the inner tissue was less severe than that of the surface tissue (He et al., 2020). For inner

tissue, there was no difference in MDA content between controlled and EUG-treated groups ( $P > 0.05$ ), as both of them were under a low level of  $1 \text{ mmol kg}^{-1}$ . Hence, it could be speculated that EUG treatment could remarkably delay membrane lipid peroxidation in the surface tissue of FWC by alleviating ROS damage to cell membranes.

### 3.5. ROS scavenging enzyme activities analysis

Plants generally utilize very efficient enzymatic pathways to protect cells from ROS damage by scavenging ROS (Chapman et al., 2019). SOD can catalyze the dismutation of  $O_2^-$  to  $H_2O_2$ , which is further decomposed into  $H_2O$  by CAT and APX, thus alleviating oxidative damage to plant tissue (Chen et al., 2019; Mhamdi et al., 2012). It is noted that APX removes  $H_2O_2$  in a different way than CAT does. To be specific, APX could reduce  $H_2O_2$  with ascorbate acting as an electron donor in the ascorbate–glutathione (ASC-GSH) cycle (Farooq et al., 2019).

As shown in Fig. 4A, SOD activities in surface tissue of untreated samples increased progressively as time was prolonged. This might be due to mechanical injury inducing the increase of SOD activity in order to reduce oxidative damage (Pan et al., 2020). SOD activity of the 1.5 % EUG-treated group was significantly higher than that of the control sample during the whole storage (except day 6), indicating that a high concentration of EUG treatment had an activation effect on SOD activities in surface tissue of FWC ( $P < 0.05$ ). Jin et al. (2012) also found that other essential oils (including carvacrol and cinnamaldehyde) at a concentration of  $1 \mu\text{L L}^{-1}$  could enhance SOD activity in Chinese bayberries. In addition, the increasing trend of SOD activities in the inner tissue of EUG-treated groups was more evident than that of the control sample (Fig. 4B). However, statistical analysis revealed that SOD activities of EUG-treated groups were significantly higher than that of the control samples, only on day 8 ( $P < 0.05$ ). These results suggested that the activation effect of EUG treatment on SOD activities in surface tissue of FWC was better than that in inner tissue.

As shown in Fig. 4C, CAT activity of controlled group increased from day 0 to day 4, which may be attributed to the induction effect of injury stress. Compared to the control, significantly higher CAT activities in the 0.4 % EUG-treated samples were observed from day 0 to day 6 ( $P < 0.05$ ). Whereas CAT activity in 1.5 % EUG-treated sample dramatically increased during the first two days of storage, and then a sudden decrease was observed. The rapid change in CAT activity was also reported by You et al. (2012). It was speculated that 1.5 % EUG treatment could accelerate the generation and consumption of peroxides and free radicals in FWC, leading to the obvious change of CAT activity (Pan et al., 2020). As shown in Fig. 4D, CAT activity in controlled group was characterized by a trend of increasing (before day 2) and then decreasing. Inner tissue of control and 0.4 % EUG-treated samples showed no difference in CAT activity during the whole storage ( $P > 0.05$ ). Besides, the obvious change of CAT activity in 1.5 % EUG-treated sample was also observed in the inner tissue.

As shown in Fig. 4E, APX activities of surface tissue in both control and EUG treated groups decreased gradually during storage, which was in concordance with the report of Dou et al. (2021). However, compared to the control and 0.4 % EUG-treated group, significantly higher APX activity was observed in 1.5 % EUG-treated samples during storage days of 2 to 8. These results suggested that 1.5 % EUG treatment could effectively enhance the  $H_2O_2$ -scavenging ability of the surface tissue of FWC, which is consistent with the findings of Jin et al. (2012). As shown in Fig. 4F, APX activities in the inner tissue of EUG-treated groups were significantly lower than that of the control on day 0 ( $P < 0.05$ ), indicating that EUG treatment could inhibit the activation effect of injury stress on APX activity of inner tissue (Chapman et al., 2019). Overall, APX activities in inner tissue of 1.5 % EUG-treated group were significantly higher than that of control during day 4 to day 8 of storage ( $P < 0.05$ ). Therefore, it can be concluded that a higher concentration (1.5 %) of EUG treatment had an activation effect on APX activities in inner tissue of FWC after four days of storage.



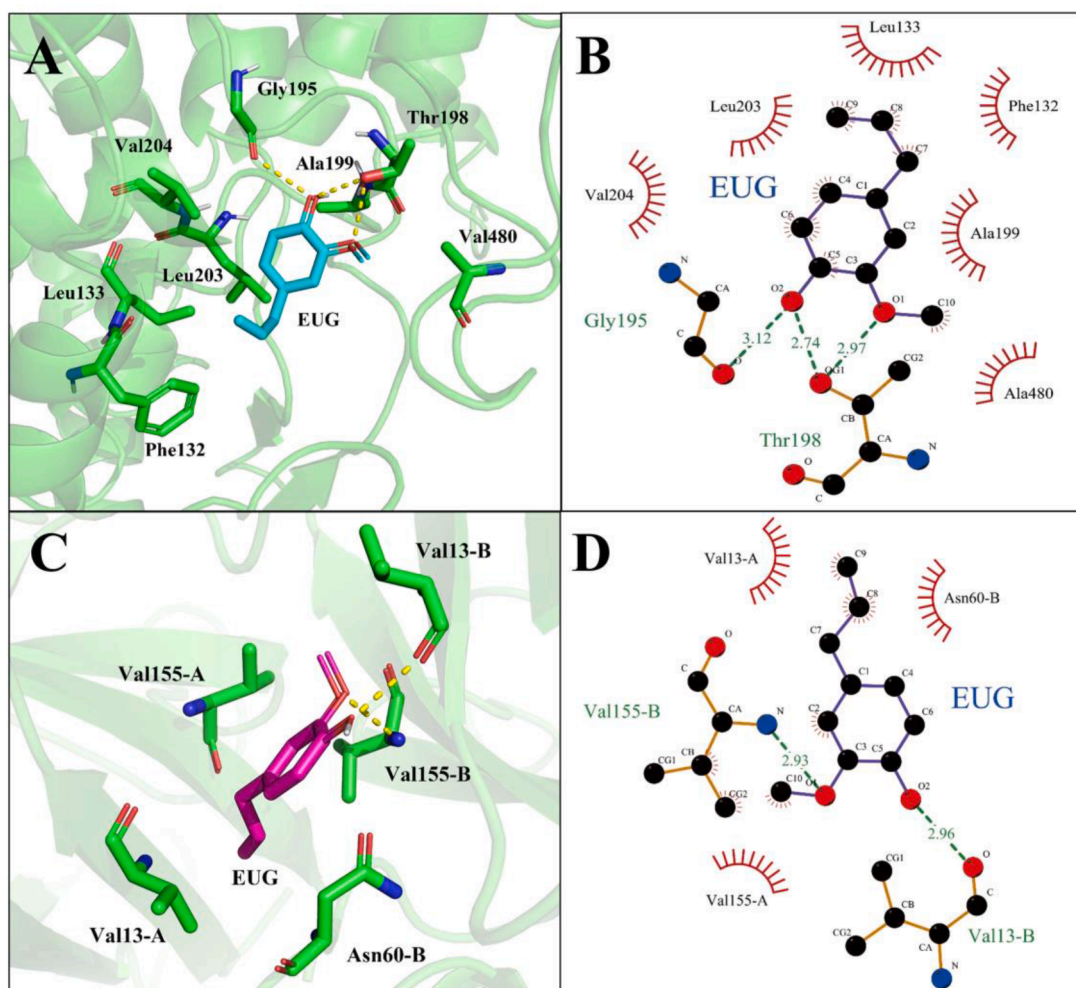


**Fig. 5.** (A) Three-dimensional map of interaction between eugenol and phenylalanine ammonia-lyase (PAL). The blue stick structure represents eugenol while the rest of green structures show the residues of PAL. (B) Two-dimensional ligand interaction map of eugenol docking with PAL. The red circle indicates hydrophobic interaction, and the green dotted line indicates hydrogen bonding. (C) Three-dimensional map of interaction between eugenol and superoxide dismutase (SOD). The purple stick structure represents eugenol while the rest of green structures show the residues of SOD. (D) Two-dimensional ligand interaction map of eugenol docking with SOD. The red circle indicates hydrophobic interaction, and the green dotted line indicates hydrogen bonding.

This study demonstrated that 1.5 % EUG treatment could remarkably keep higher levels of SOD, CAT and APX activities in the surface tissue of FWC (during the whole storage). The EUG treatment could increase SOD and APX activities in the inner tissue of treated FWC during the late-storage period. Similarly, Zhang et al. (2018) found that the delayed browning in litchi fruit might be due to the melatonin treatment which could enhance the anti-oxidative processes via activating SOD, CAT and APX. Thus, the enhanced ROS-scavenging enzyme activities and reduced membrane lipid peroxidation might be involved to cause browning inhibition of EUG-treated FWC.

### 3.6. Molecular docking analysis

One of the browning-related enzymes and one of the ROS-scavenging enzymes were selected to conduct molecular docking in order to analyze the direct effect of EUG on enzymes. PAL was chosen to represent the browning-related enzymes because EUG had the best inhibition effect on it (Fig. 2), and it had a significantly positive correlation with browning degree in FWC (Table S1). SOD was chosen to represent the ROS-scavenging enzymes because EUG had the best activation effect on it (Fig. 4), and it was the initial enzyme for scavenging ROS (Chen et al., 2019).

The conformation between PAL and EUG with the lowest binding

energy ( $-4.9 \text{ kcal mol}^{-1}$ ) was selected as the best docking result. The active center of PAL had highly conserved Ala-Ser-Gly residues, which could dehydrate to form the 4-methylidene-imidazole-5-one (MIO) and bind to the substrate L-Phe (Ritter & Schulz, 2004). The EUG-binding residues close to MIO of PAL were identified in our current study. As shown in Fig. 5A and 5B, EUG interacted with the active site of PAL mainly through hydrophobic interaction and the residues involved included Phe132, Leu133, Ala199, Leu203, Val204 and Ala480. Notably, three hydrogen bonding interactions were observed between EUG and the residues, including Gly195 (bond length:  $3.12 \text{ \AA}$ ) and Thr198 (bond length:  $2.74 \text{ \AA}$ ,  $2.97 \text{ \AA}$ ) (Table S2). Chen et al. (2017) reported that EUG could interact with Asn260 and Asn384 residues of the PAL active site of fresh-cut lettuce, thereby inhibiting the binding of PAL to its substrate L-Phe. Hence, it is concluded that the above interactions between EUG and the active site of PAL could prevent the formation of cinnamic acid and its downstream products.

The optimal molecular docking result between EUG and SOD with the lowest binding energy ( $-5.7 \text{ kcal mol}^{-1}$ ) was displayed in Fig. 5C and 5D. There are two subunits in SOD crystal structure, which are tightly joined by hydrophobic and electrostatic forces (Tainer, Getzoff, Richardson, & Richardson, 1983). Two hydrogen bondings with bond lengths of  $2.96 \text{ \AA}$  and  $2.93 \text{ \AA}$  were formed between EUG and the residues Val13 and Val155 of chain B of SOD (Fig. 5D and Table S2). At the same

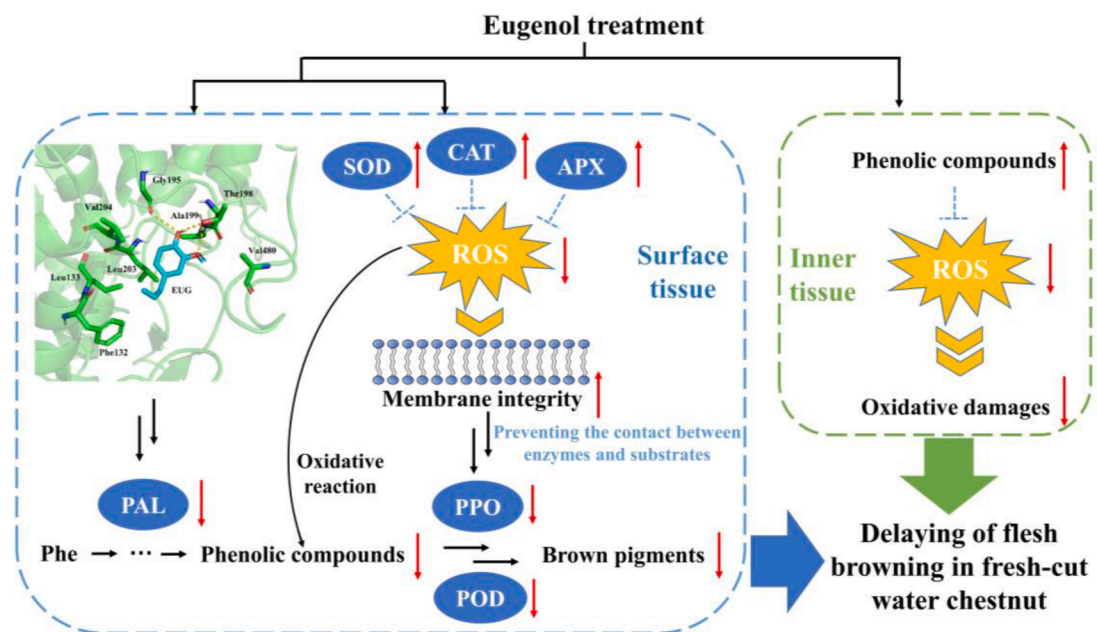


Fig. 6. The possible mechanism of eugenol treatment delaying flesh browning in fresh-cut water chestnut via inhibiting phenylalanine ammonia-lyase activity and regulating reactive oxygen species metabolism in surface tissue and inner tissue of fresh-cut water chestnut.

time, EUG was found to interact with the residues (Val13-A, Asn60-B, Val155-A) of SOD by hydrophobic interactions. The binding sites of EUG to SOD were located in the middle of the two subunits, which were away from the active site of SOD. A previous study has also reported that cadmium increased the SOD activity by binding around the surface residues of SOD (Wang et al., 2015). Hence, we can also speculate that the interactions between EUG and surface residues of SOD might change the conformation of SOD, further facilitating  $O_2^-$  to enter the active sites.

### 3.7. Proposed mechanism of EUG inhibiting browning of FWC

The possible mechanism of browning inhibition in FWC after EUG treatment was illustrated in Fig. 6. EUG treatment could notably inhibit the PAL activity and reduce the phenols content. Molecular docking studies confirmed that EUG could bind the residues of the PAL active site through hydrophobic interactions and hydrogen bondings. Therefore, EUG treatment was found to cause a direct inhibitory effect on PAL activity of surface tissue, which could contribute to the retardation of phenols accumulation and following discoloration in the surface tissue of FWC. Moreover, EUG treatment could directly inhibit enzymatic browning by suppressing PPO/POD activity and reducing ROS content. Furthermore, EUG treatment could also induce evident enhancement in the enzymatic and non-enzymatic antioxidant systems, thereby, indirectly inhibiting enzymatic browning of FWC. For surface tissue, EUG treatment could enhance its antioxidant capacity by increasing ROS-scavenging enzymes (including SOD, CAT and APX) activities. Thus, an increase in antioxidant capacity could alleviate oxidative damage to cell membranes, which might contribute to the prevention of the contact between phenols and oxidative enzymes (PPO/POD) and subsequent enzymatic browning in surface tissue. For inner tissue, EUG treatment could increase its antioxidant capacity and sustain cellular membrane integrity by inducing the generation of phenolic compounds with antioxidant ability. Hence, the browning inhibition in FWC after EUG treatment might be attributed to the direct inhibitory effect on PAL activity and the indirect enhancement of antioxidant capacity in both surface and inner tissues through enzymatic or non-enzymatic ways.

## 4. Conclusions

Effect of EUG treatment (with concentrations of 0.4 % and 1.5 %, dipping for 60 s) on browning in FWC and its possible mechanism was investigated. EUG treatment had positive effects on browning inhibition in FWC. 1.5 % EUG treatment was found to be more favorable than 0.4 % EUG for inhibiting browning in FWC. This browning inhibition in FWC after EUG treatment was found to be associated with its direct inhibitory effect on PAL activities and the retardation of the subsequent accumulation of yellow phenols on the surface tissue. Moreover, EUG treatment could enhance the ROS-scavenging enzyme (including SOD, CAT, and APX) activities in surface tissue and increase phenolic content in inner tissue, which also contributed to the alleviation of oxidative damage to cell membranes and inhibition of enzymatic browning. Therefore, EUG treatment could be applied as a promising technology for inhibiting browning and extending the shelf life of FWC.

### Funding

This work was supported by the Fundamental Research Funds for the Central Universities (2662018JC018, 2662020SPPY012); and the National Natural Science Foundation of China(31401507); and a Hubei Province Technical Innovation Special Major Project (2018ABA072); and the National Key Research and Development Program (2017YFD0400701-2).

### Declaration of Competing Interest

The authors declare that they have no known competing financial interests or personal relationships that could have appeared to influence the work reported in this paper.

### Appendix A. Supplementary data

Supplementary data to this article can be found online at <https://doi.org/10.1016/j.fochx.2022.100307>.

### References

- Boudet, A. M. (2007). Evolution and current status of research in phenolic compounds. *Phytochemistry*, 68(22–24), 2722–2735. <https://doi.org/10.1016/j.phytochem.2007.06.012>

- Chapman, J. M., Muhlemann, J. K., Gayomba, S. R., & Muday, G. K. (2019). RBOH-Dependent ROS Synthesis and ROS Scavenging by Plant Specialized Metabolites to Modulate Plant Development and Stress Responses. *Chemical Research in Toxicology*, 32(3), 370–396. <https://doi.org/10.1021/acs.chemrestox.9b00028>
- Chen, X., Ren, L., Li, M., Qian, J., Fan, J., & Du, B. (2017). Effects of clove essential oil and eugenol on quality and browning control of fresh-cut lettuce. *Food Chemistry*, 214, 432–439. <https://doi.org/10.1016/j.foodchem.2016.07.101>
- Chen, Y., Hung, Y. C., Chen, M., Lin, M., & Lin, H. (2019). Enhanced storability of blueberries by acidic electrolyzed oxidizing water application may be mediated by regulating ROS metabolism. *Food Chemistry*, 270, 229–235. <https://doi.org/10.1016/j.foodchem.2018.07.095>
- Concellón, A., Zaro, M. J., Chaves, A. R., & Vicente, A. R. (2012). Changes in quality and phenolic antioxidants in dark purple American eggplant (*Solanum melongena* L. cv. Lucia) as affected by storage at 0°C and 10°C. *Postharvest Biology and Technology*, 66, 35–41. <https://doi.org/10.1016/j.postharvbio.2011.12.003>
- Das, K., & Roychoudhury, A. (2014). Reactive oxygen species (ROS) and response of antioxidants as ROS-scavengers during environmental stress in plants. *Frontiers in Environmental Science*, 2, 1–13. <https://doi.org/10.3389/fenvs.2014.00053>
- Dou, Y., Chang, C., Wang, J., Cai, Z., Zhang, W., Du, H., ... Zhu, L. (2021). Hydrogen Sulfide Inhibits Enzymatic Browning of Fresh-Cut Chinese Water Chestnuts. *Frontiers in Nutrition*, 8, 1–9. <https://doi.org/10.3389/fnut.2021.652984>
- Farooq, M. A., Niazi, A. K., Akhtar, J., Saifullah, F., & M., Souri, Z., Rengel, Z. (2019). Acquiring control: The evolution of ROS-Induced oxidative stress and redox signaling pathways in plant stress responses. *Plant Physiology and Biochemistry*, 141, 353–369. <https://doi.org/10.1016/j.plaphy.2019.04.039>
- Feumba, R., Panyoo, E., & P. A. R., Metsatedem, Q., Moses, C., & Mbofung, F. (2020). Effect of microwave blanching on antioxidant activity, phenolic compounds and browning behaviour of some fruit peelings. *Food Chemistry*, 302, Article 125308. <https://doi.org/10.1016/j.foodchem.2019.125308>
- Finkel, T. (2011). Signal transduction by reactive oxygen species. *Journal of Cell Biology*, 194(1), 7–15. <https://doi.org/10.1083/jcb.201102095>
- Gong, L., Li, T., Chen, F., Duan, X., Yuan, Y., Zhang, D., & Jiang, Y. (2016). An inclusion complex of eugenol into  $\beta$ -cyclodextrin: Preparation, and physicochemical and antifungal characterization. *Food Chemistry*, 196, 324–330. <https://doi.org/10.1016/j.foodchem.2015.09.052>
- He, F., & Pan, Y. (2017). Purification and characterization of chalcone isomerase from fresh-cut Chinese water-chestnut. *LWT - Food Science and Technology*, 79, 402–409. <https://doi.org/10.1016/j.lwt.2017.01.034>
- He, M., Ge, Z., Hong, M., Hongxia, Q., Duan, X., Ze, Y., ... Jiang, Y. (2020). Alleviation of pericarp browning in harvested litchi fruit by synephrine hydrochloride in relation to membrane lipids metabolism. *Postharvest Biology and Technology*, 166, Article 111223. <https://doi.org/10.1016/j.postharvbio.2020.111223>
- Jin, P., Wu, X., Xu, F., Wang, X., Wang, J., & Zheng, Y. (2012). Enhancing antioxidant capacity and reducing decay of Chinese bayberries by essential oils. *Journal of Agricultural and Food Chemistry*, 60, 3769–3775. <https://doi.org/10.1021/jf300151n>
- Jing, Y., Huang, J., & Yu, X. (2019). Maintenance of the antioxidant capacity of fresh-cut pineapple by procyandin-grafted chitosan. *Postharvest Biology and Technology*, 154, 79–86. <https://doi.org/10.1016/j.postharvbio.2019.04.022>
- Kim, J. G., Kim, H. L., Kim, S. J., & Park, K. (2013). Fruit quality, anthocyanin and total phenolic contents, and antioxidant activities of 45 blueberry cultivars grown in Suwon, Korea. *Journal of Zhejiang University-SCIENCE B (Biomedicine & Biotechnology)*, 14(9), 793–799. <https://doi.org/10.1631/jzus.B1300012>
- Kong, M., Murtaza, A., Hu, X., Iqbal, A., Zhu, L., Ali, S. W., ... Hu, W. (2021). Effect of high-pressure carbon dioxide treatment on browning inhibition of fresh-cut Chinese water chestnut (*Eleocharis tuberosa*): Based on the comparison of damaged tissue and non-damaged tissue. *Postharvest Biology and Technology*, 179(1), Article 111557. <https://doi.org/10.1016/j.postharvbio.2021.111557>
- Li, F., Hu, Y., Shan, Y., Liu, J., Ding, X., Duan, X., ... Jiang, Y. (2022). Hydrogen-rich water maintains the color quality of fresh-cut Chinese water chestnut. *Postharvest Biology and Technology*, 183, Article 111743. <https://doi.org/10.1016/j.postharvbio.2021.111743>
- Liu, H., Jiang, W., Cao, J., & Li, Y. (2019). Effect of chilling temperatures on physiological properties, phenolic metabolism and antioxidant level accompanying pulp browning of peach during cold storage. *Scientia Horticulturae*, 255, 175–182. <https://doi.org/10.1016/j.scienta.2019.05.037>
- Martinez-Hernandez, E., Cui, X., Scown, C. D., Amezcua-Allieri, M. A., Aburto, J., & Simmons, B. A. (2019). Techno-economic and greenhouse gas analyses of lignin valorization to eugenol and phenolic products in integrated ethanol biorefineries. *Biofuels, Bioproducts and Biorefining*, 13(4), 978–993. <https://doi.org/10.1002/bbb.1989>
- Mhamdi, A., Noctor, G., & Baker, A. (2012). Plant catalases: Peroxisomal redox guardians. *Archives of Biochemistry and Biophysics*, 525(2), 181–194. <https://doi.org/10.1016/j.abb.2012.04.015>
- Pan, Y., Chen, L., Pang, L., Chen, X., Jia, X., & Li, X. (2020). Ultrasound treatment inhibits browning and improves antioxidant capacity of fresh-cut sweet potato during cold storage. *RSC Advances*, 10(16), 9193–9202. <https://doi.org/10.1039/c9ra06418d>
- Pan, Y. G., Li, Y. X., & Yuan, M. Q. (2015). Isolation, purification and identification of etiolation substrate from fresh-cut Chinese water-chestnut (*Eleocharis tuberosa*). *Food Chemistry*, 186, 119–122. <https://doi.org/10.1016/j.foodchem.2015.03.070>
- Perumal, A. B., Sellamuthu, P. S., Nambiar, R. B., & Sadiku, E. R. (2017). Effects of Essential Oil Vapour Treatment on the Postharvest Disease Control and Different Defence Responses in Two Mango (*Mangifera indica* L.) Cultivars. *Food and Bioprocess Technology*, 10(6), 1131–1141. <https://doi.org/10.1007/s11947-017-1891-6>
- Ritter, H., & Schulz, G. E. (2004). Structural basis for the entrance into the phenylpropanoid metabolism catalyzed by phenylalanine ammonia-lyase. *Plant Cell*, 16, 3426–3436. <https://doi.org/10.1105/tpc.104.025288>
- Sharifmehar, S., Soltanizadeh, N., & Goli, S. A. H. (2019). Physicochemical properties of fried shrimp coated with bio-nano-coating containing eugenol and Aloe vera. *Lwt*, 109, 33–39. <https://doi.org/10.1016/j.lwt.2019.03.084>
- Song, M., Shuai, L., Huang, S., Wu, S., Cao, X., Duan, Z., ... Fang, F. (2019a). RNA-Seq analysis of gene expression during the yellowing developmental process of fresh-cut Chinese water chestnuts. *Scientia Horticulturae*, 250, 421–431.
- Song, M., Wu, S., Shuai, L., Duan, Z., Chen, Z., Shang, F., & Fang, F. (2019b). Effects of exogenous ascorbic acid and ferulic acid on the yellowing of fresh-cut Chinese water chestnut. *Postharvest Biology and Technology*, 148, 15–21. <https://doi.org/10.1016/j.postharvbio.2018.10.005>
- Sun, J., Lin, H., Zhang, S., Lin, Y., Wang, H., Lin, M., & Chen, Y. (2018). The roles of ROS production-scavenging system in *Lasioidiplodia theobromae* (Pat.) Griff. & Maubl.-induced pericarp browning and disease development of harvested longan fruit. *Food Chemistry*, 247, 16–22. <https://doi.org/10.1016/j.foodchem.2017.12.017>
- Sun, Y., Sun, H., Luo, M., Zhou, X., Zhou, Q., Wei, B., ... Ji, S. (2020). Membrane lipid metabolism in relation to core browning during ambient storage of 'Nanguo' pears. *Postharvest Biology and Technology*, 169, Article 111288. <https://doi.org/10.1016/j.postharvbio.2020.111288>
- Surjadinata, B. B., & Cisneros-Zevallos, L. (2012). Biosynthesis of phenolic antioxidants in carrot tissue increases with wounding intensity. *Food Chemistry*, 134, 615–624. <https://doi.org/10.1016/j.foodchem.2012.01.097>
- Tainer, J. A., Getzoff, E. D., Richardson, J. S., & Richardson, D. C. (1983). Structure and mechanism of copper, zinc superoxide dismutase. *Nature*, 306, 284–287. <https://doi.org/10.1038/306284a0>
- Teng, Y., Murtaza, A., Iqbal, A., Fu, J., Ali, S. W., Iqbal, M. A., ... Hu, W. (2020). Eugenol emulsions affect the browning processes, and microbial and chemical qualities of fresh-cut Chinese water chestnut. *Food Bioscience*, 38, Article 100716. <https://doi.org/10.1016/j.fbio.2020.100716>
- Trott, O., & Olson, A. J. (2010). AutoDock Vina: Improving the speed and accuracy of docking with a new scoring function, efficient optimization, and multithreading. *Journal of Computational Chemistry*, 31(2), 455–461. <https://doi.org/10.1002/jcc.21334>
- Wang, J., Zhang, H., Zhang, T., Zhang, R., Liu, R., & Chen, Y. (2015). Molecular mechanism on cadmium-induced activity changes of catalase and superoxide dismutase. *International Journal of Biological Macromolecules*, 77, 59–67. <https://doi.org/10.1016/j.ijbiomac.2015.02.037>
- Wieczyńska, J., & Cavoski, I. (2018). Antimicrobial, antioxidant and sensory features of eugenol, carvacrol and trans-anethole in active packaging for organic ready-to-eat iceberg lettuce. *Food Chemistry*, 259, 251–260. <https://doi.org/10.1016/j.foodchem.2018.03.137>
- You, Y., Jiang, Y., Sun, J., Liu, H., Song, L., & Duan, X. (2012). Effects of short-term anoxia treatment on browning of fresh-cut Chinese water chestnut in relation to antioxidant activity. *Food Chemistry*, 132(3), 1191–1196. <https://doi.org/10.1016/j.foodchem.2011.11.073>
- Zeng, R., Zhang, A., Chen, J., & Fu, Y. (2012). Postharvest quality and physiological responses of clove bud extract dip on "Newhall" navel orange. *Scientia Horticulturae*, 138, 253–258. <https://doi.org/10.1016/j.scienta.2012.02.036>
- Zhang, Y., Huber, D. J., Hu, M., Jiang, G., Gao, Z., Xu, X., ... Zhang, Z. (2018). Delay of Postharvest Browning in Litchi Fruit by Melatonin via the Enhancing of Antioxidative Processes and Oxidation Repair. *Journal of Agricultural and Food Chemistry*, 66, 7475–7484. <https://doi.org/10.1021/acs.jafc.8b01922>
- Zhou, D., Wei, Y., Peng, J., Tu, S., Wang, Z., & Tu, K. (2019). Carvacrol and eugenol inhibit postharvest soft rot disease by enhancing defense response in peaches during storage. *Journal of Food Processing and Preservation*, 43, Article e14086. <https://doi.org/10.1111/jfpp.14086>